

Small-Angle Neutron Scattering Study of Temperature-Induced Structural Changes in Liposomes

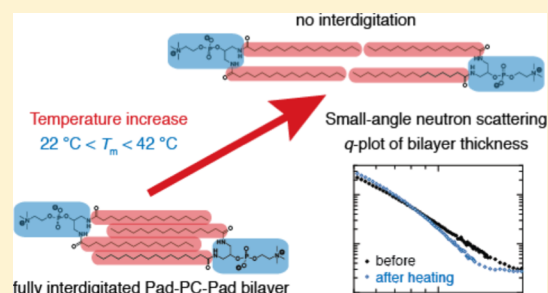
Sofiya Matviyukiv,[†] Hans Deyhle,^{†,||} Joachim Kohlbrecher,[‡] Frederik Neuhaus,[§] Andreas Zumbuehl,[§] and Bert Müller^{*,†,‡,§}

[†]Biomaterials Science Center, Department of Biomedical Engineering, University of Basel, Allschwil 4123, Switzerland

[‡]Laboratory for Neutron Scattering and Imaging, Paul Scherrer Institute, Villigen PSI 5232, Switzerland

[§]National Center of Competence in Research in Chemical Biology, Geneva 1211, Switzerland

ABSTRACT: Liposomes of specific artificial phospholipids, such as Pad-PC-Pad and Rad-PC-Rad, are mechanically responsive. They can release encapsulated therapeutics via physical stimuli, as naturally present in blood flow of constricted vessel segments. The question is how these synthetic liposomes change their structure in the medically relevant temperature range from 22 to 42 °C. In the present study, small-angle neutron scattering (SANS) was employed to evaluate the temperature-induced structural changes of selected artificial liposomes. For Rad-PC-Rad, Pad-Pad-PC, Sur-PC-Sur, and Sad-PC-Sad liposomes, the SANS data have remained constant because the phase transition temperatures are above 42 °C. For Pad-PC-Pad and Pes-PC-Pes liposomes, whose phase transitions are below 42 °C, the *q*-plots have revealed temperature-dependent structural changes. The average diameter of Pad-PC-Pad liposomes remained almost constant, whereas the eccentricity decreased by an order of magnitude. Related measurements using transmission electron microscopy at cryogenic temperatures, as well as dynamic light scattering before and after the heating cycles, underpin the fact that the non-spherical liposomes flatten out. The SANS data further indicated that, as a consequence of the thermal loop, the mean bilayer thickness increased by 20%, associated with the loss of lipid membrane interdigitation. Therefore, Pad-PC-Pad liposomes are unsuitable for local drug delivery in the atherosclerotic human blood vessel system. In contrast, Rad-PC-Rad liposomes are thermally stable for applications within the human body.



INTRODUCTION

Liposomes are composed of lipid bilayers and usually have a spherical shape.¹ Using artificial phospholipids with a dedicated backbone chemistry and tail length that form interdigitated bilayers, faceted liposomes have been discovered.² These liposomes are beneficial in medical therapies because they possess distinctive characteristics. As conventional liposomes, they can encapsulate therapeutic molecules and transport them to the desired location, preventing direct contact between drug and blood. Upon mechanical stimuli, however, these liposomes can undergo structural changes to release the cargo.³ In this manner, the totally administered dose and the related objectionable side effects along the patient's 60 000-miles-long blood vessel system being currently flooded with the drug can be kept extremely low, whereas the purely physical trigger renders possible an unrivaled local dose to pathological constrictions.

The thermal stability of these faceted liposomes within the physiologically relevant temperature range, however, has hardly been studied yet. It is well known that the body temperature is generally close to 37 °C. On grounds of ill health, the body temperatures can raise to above 40 °C, but at a temperature of 42 °C the circulation fails. Hypothermia, as, for example, intentionally induced during heart surgery, gives rise to body

temperatures close to 20 °C.⁴ Therefore, the present study covers the temperature range between 22 and 42 °C.

The size and shape of liposomes including their distributions can be assessed by employing dynamic light scattering (DLS) and cryogenic transmission electron microscopy (cryo-TEM). For the structural characterization of the lipid bilayer thickness, however, a technique with better resolving power is needed. Therefore, we applied small-angle neutron scattering (SANS) as a tool to obtain quantitative information about the structural parameters of liposomes as the function of temperature. SANS allows for the investigation of fully hydrated systems, offering the additional feature of contrast variation via solvent exchange. More importantly, our setup was equipped with a heating stage to conveniently control the temperature of the liposomal suspensions within the medically relevant range.

Liposomes from DPPC exhibit a spherical shape. Non-spherical shapes can be obtained replacing the 1,2- by the 1,3-arrangement of the fatty acyl chains in the backbone as found in Pad-PC-Pad, Rad-PC-Rad, Pes-PC-Pes, Sur-PC-Sur, and Sad-PC-Sad, see Figures 1 and 2 below. This arrangement increases the spacing between the chains and leads to

Received: May 28, 2019

Revised: July 19, 2019

Published: July 25, 2019

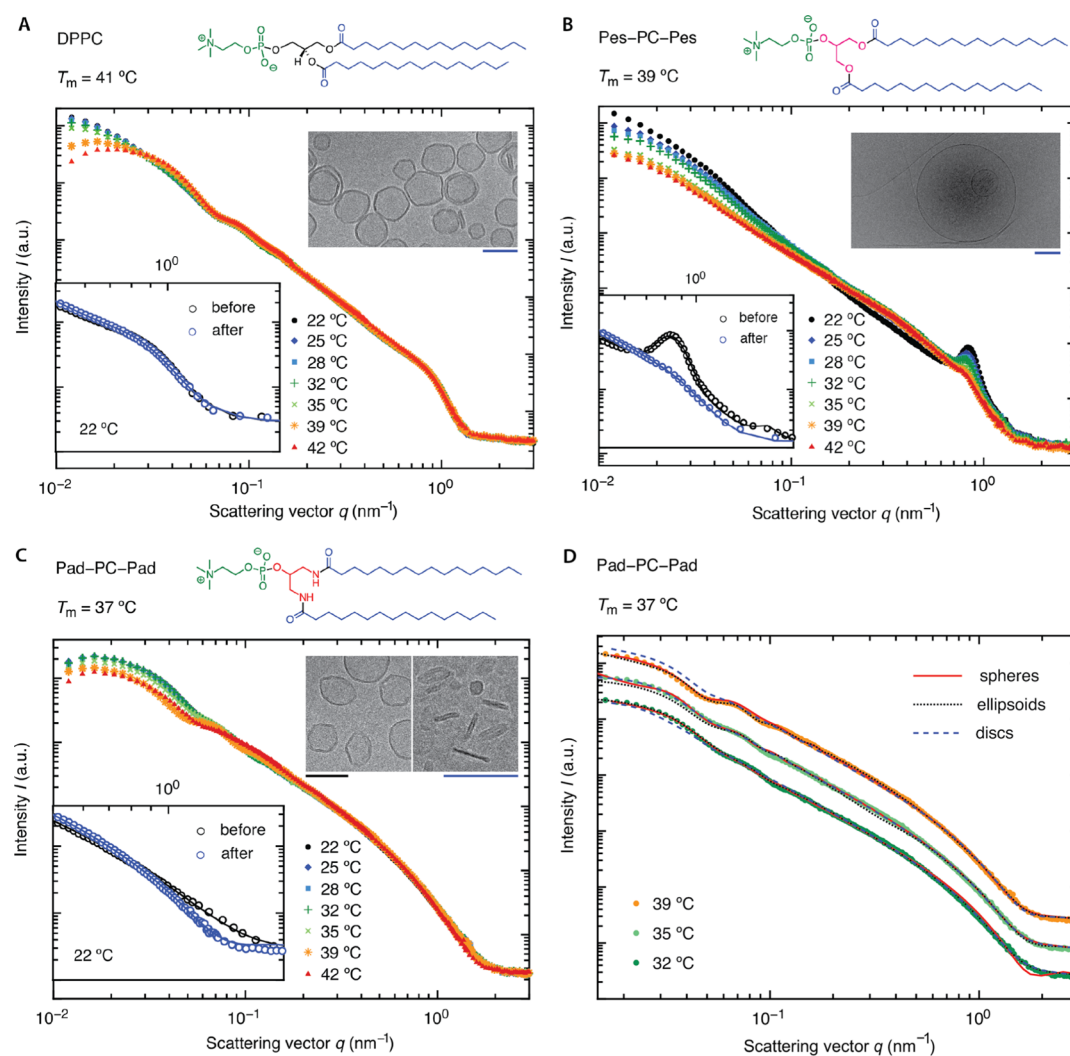


Figure 1. SANS data and related cryo-TEM images of liposomal suspensions reveal temperature-induced structural changes close to their transition temperatures T_m . The structural representations of the phospholipids show color-coded chemical motives. The inset diagrams display the scattering signal for higher q -values, before (black circles) and after (blue circles) heating and the related fits using the generalized Guinier law. The scale bars of the TEM micrographs correspond to 100 nm, where black and blue indicate imaging was recorded before and after the heating cycle, respectively. Diagram (D) provides the reader an idea how far the liposomes can be approximated by spheres, ellipsoids, or discs. The goodness of fit, described by reduced chi-square, is for the spheres 91.2, 30.1, 51.0, for the ellipsoids 21.7, 178.7, 17.6, and for the discs 65.4, 18.3, 237.0 at the temperatures 32, 35 and 39 °C, respectively. To suitably visualize the differences, the values for 35 and 39 °C were shifted with respect to those for 32 °C along the ordinate by a factor of three and 10, respectively.

interdigitated lipids in the membrane. Longer carbon chains improve the thermal stability by increasing the hydrophobic forces between the chains, revealed by an increase in the transition temperature. Because this class of liposomes has substantially stiffer lipid bilayers than the established natural membranes, faceted liposomes with specific defects and related mechanical features can be tailored. Pad-PC-Pad and Rad-PC-Rad as well as the less reported Pes-PC-Pes, Pad-Pad-PC, Sur-PC-Sur, and Sad-PC-Sad lipids belong to a family that forms metastable non-spherical liposomes. Their interdigitated lipid bilayers are thinner and more rigid than the conventional ones such as the well-established DPPC liposomes. They exhibit a distinct curvature in only one direction associated with defect lines. Therefore, these non-spherical liposomes represent a metastable state, and the application of mechanical or thermal energy can result in structural changes. The mechanical stimulation was already studied in some detail,⁵ whereas the thermal characterization was mainly restricted to

the measurement of the main membrane phase transition temperature from a gel to the liquid crystalline phase.^{3,6}

In this study, we detect temperature-dependent changes in the size, shape, and bilayer properties of liposomal formulations, composed of the family of selected artificial phospholipids, and, in this regard, the structural changes at medically relevant body temperatures are of particular interest.

MATERIALS AND METHODS

Liposome Preparation. The lipids were synthesized as reported.^{3,6–9} The liposomes were formulated following the standard extrusion protocol.¹⁰ Briefly, 10 mg of lipids were dissolved in CH_2Cl_2 . After evaporating the organic solvent, the thin film was dried further under vacuum conditions with a pressure of 40 mbar overnight. The film was hydrated with D_2O for a period of 30 min. Five freeze–thaw cycles from liquid nitrogen temperature to 65 °C were carried out and followed by eleven extrusion cycles, using a Mini Extruder (Avanti Polar Lipids, USA) and track-edged filters with

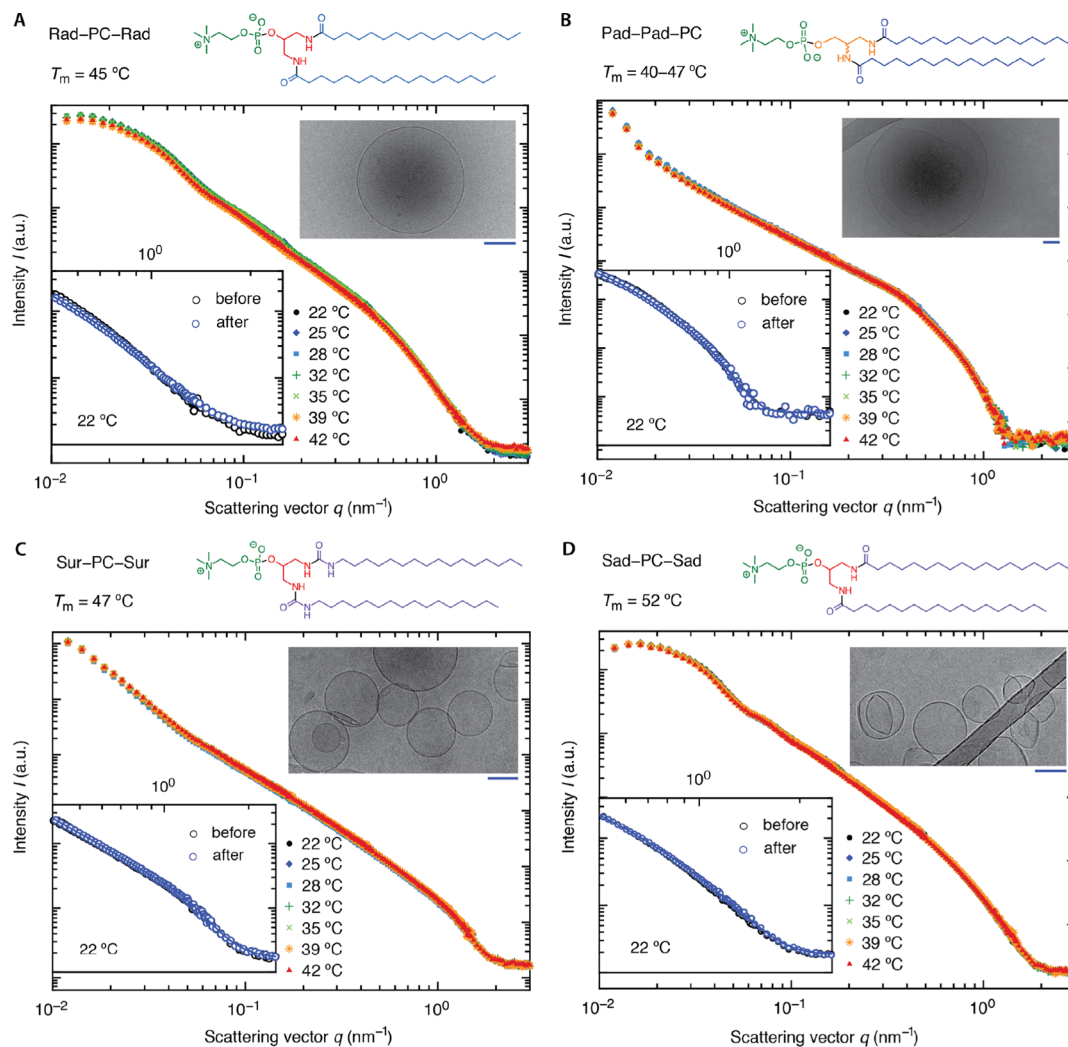


Figure 2. SANS data and cryo-TEM images of Rad-PC-Rad, Pad-Pad-PC, Sur-PC-Sur, and Sad-PC-Sad liposomes hardly show any thermal effect, because the transition temperatures T_m are above the medically relevant range. The structural representations of the phospholipids show color-coded chemical motives, i.e. the C16 chain—dark blue, the C17 chain—light blue, and the C18 chain—purple. The inset diagrams display the scattering signal for higher q -values, before (black circles) and after (blue circles) heating and the related fits using the generalized Guinier law. The scale bars of the micrographs correspond to 100 nm.

100 nm pore size (Whatman, USA). The obtained liposomal formulations exhibited a lipid concentration of about 10 mg/mL.

Dynamic Light Scattering. The DLS traces were measured using the DelsaMax PRO apparatus (Beckman Coulter, USA). Here, the photodiode is positioned at 168° backscatter angle and detector position at 163.5° associated with scattering angles ranging from 4 to 15° . The measurements were carried out at room temperature and at a lipid concentration of 0.3 mg/mL in D_2O . The data were averaged among five independent measurements before heating cycles and three measurements eight months after applying the heating cycles. The data were treated with the cumulant analysis method.

cryo-Transmission Electron Microscopy. The liposomal suspensions were diluted at a ratio of 1:2 with D_2O and thus to a concentration of 5 mg/mL. Next, 4 μ L aliquots of each suspension were adsorbed onto a holey carbon-coated grid (Lacey, Ted Pella, USA), blotted with Whatman 1 filter paper and vitrified into liquid ethane at a temperature of $-178^\circ C$, using a Leica GP plunger (Leica, Austria). Frozen grids were transferred onto a Talos electron microscope (Thermo Fisher, USA), using a Gatan 626 cryo-holder. Electron micrographs were recorded at an accelerating voltage of 200 kV and a nominal magnification of 45 000 \times , using a low-dose system (0.20 e^-/nm^2) and keeping the sample at liquid nitrogen temperature. Micrographs were recorded on the CETA camera. Pixel size at the sample level was (0.326 nm) 2 . Because some of the cryo-

TEM micrographs exhibited slowly varying brightness variations, we compensated for such artefacts using a modified fuzzy C-means algorithm.^{11,12}

Small-Angle Neutron Scattering. The SANS measurements were performed at the SANS-I facility, Swiss Spallation Neutron Source SINQ, Paul Scherrer Institute, Switzerland. Neutrons with an energy of 400 meV, which corresponds to a wavelength λ of 0.045 nm, were used at sample-to-detector distances of 1.6, 6.0, and 18.0 m and exposure times of 190 and 564 s. In addition, neutrons with an energy of 60 meV ($\lambda = 0.12$ nm) at a sample-to-detector distance of 18.0 m and an exposure time of 950 s were employed. The wavelength's spread was about 10%. This choice of parameters allowed for the data collection over the range of scattering vectors q between 0.01 and 10 nm^{-1} , required to observe both the global size and shape of liposomes as well as their membrane thickness. The samples were loaded into 2 mm-path length boron-free quartz glass cells and mounted in the temperature-controlled holder. This system allows for controlling the temperature of the specimen with an accuracy better than 1 K. The liposomal suspensions were measured between 22 and 42 $^\circ C$ in 3–4 K steps. Subsequently, the suspensions were cooled down to 22 $^\circ C$ (room temperature) and measured again. The scattering data were collected with a two-dimensional 3He -detector using an array of 128 \times 128 pixels. They were radially averaged to obtain the one-dimensional $I(q)$ signals using the scattering angle θ

Table 1. Results of the Dynamic Light Scattering from the Liposomes Used^a

lipid	T_m , °C	before heating		after heating	
		size, nm	PDI	size, nm	PDI
DPPC	41	120 ± 2	0.01 ± 0.01	600 ± 40	0.33 ± 0.02
Pad-PC-Pad	37	126 ± 4	0.19 ± 0.04	53 ± 4	0.33 ± 0.04
Rad-PC-Rad	45	150 ± 3	0.57 ± 0.01	700 ± 100	0.32 ± 0.03
Pes-PC-Pes	39	170 ± 20	0.57 ± 0.01	3100 ± 200	0.92 ± 0.08
Pad-Pad-PC	40–47	1500 ± 30	0.57 ± 0.01	n.a. ^b	n.a.
Sur-PC-Sur	47	400 ± 100	0.57 ± 0.01	n.a.	n.a.
Sad-PC-Sad	52	160 ± 3	0.23 ± 0.01	220 ± 10	0.20 ± 0.02

^aThe errors originate from the standard deviations of independent measurements. ^bHere, n.a. means the data could not be extracted because of aggregate size.

$$q = \frac{4\pi}{\lambda} \sin\left(\frac{\theta}{2}\right) \quad (1)$$

The data were corrected for transmission, background scattering, and detector efficiency according to a standard procedure using the BerSANS software package.^{13,14}

Models Used for SANS Data Analysis. The SANS data were analyzed using the SASfit software¹⁵ and the implemented models. The datasets of Pad-PC-Pad and Rad-PC-Rad liposome suspensions were fitted over the entire q -range measured. Here, we used the spherical, ellipsoidal shell and discs models with a homogeneous cross-section¹⁶ and size distributions in terms of both thickness and radius. The elliptical shell model is defined by three orthogonal axes with lengths $a = b = R$ and $c = \epsilon R$, along with eccentricity $\epsilon > 0$, ($\epsilon < 1$: oblate, $\epsilon = 1$: spherical, and $\epsilon > 1$: prolate). For Pad-PC-Pad, we also included the sticky hard sphere model^{17,18} to account for inter-particle interactions, as it defines the stickiness parameter, which characterizes the adhesive strength and helps to describe liposome aggregation. The fits of the other liposomal suspensions were restricted to the q -range related to the lipid bilayer thickness. Here, we used a generalized Guinier approximation^{19,20} to extract the bilayer thickness. This approximation is extended to planar objects and based on local planes with a homogeneous cross section. It does not include any assumption of the overall shape of the liposomes and is given by

$$I(q) = \frac{2\pi}{q^2} A \exp(-R_a^2 q^2) \quad (2)$$

where A is the constant pre-factor, see for example ref 20.

The bilayer thickness t was calculated according to

$$t = \sqrt{12} R_a \quad (3)$$

The bilayer thickness is orders of magnitude smaller than the diameter of the liposomes. In such case, the form factor can be factorized.²¹ Therefore, the extraction of the bilayer thickness is allowed without loss of quality.

Multi-lamellar contributions for DPPC, Pad-Pad-PC, Pes-PC-Pes, and Sur-PC-Sur were integrated using the para-crystalline theory.^{22,23}

RESULTS

Liposome Characterization by Dynamic Light Scattering. Table 1 lists the hydrodynamic diameter and polydispersity of the liposomes before ($n = 5$) and after ($n = 3$) the thermal cycles performed for the temperature-dependent SANS measurements. The main phase transition temperatures T_m are known.^{3,6,8,9,24} In the course of the SANS experiments, the liposomes underwent heating to 42 °C and back to room temperature, which resulted in substantial changes of hydrodynamic sizes and the polydispersity indices. In general, the liposomes showed an increase in size, which could be understood by aggregation owing to the low repulsive forces between the basically neutral liposomes. The exception

was found for Pad-PC-Pad liposomes, which exhibited a decrease by a factor of two. This result for the DLS measurements was confirmed using cryo-TEM.

Small-Angle Neutron Scattering Measurements. Figures 1 and 2 summarize the temperature-dependent neutron scattering experiments for the liposomes with T_m below and above 42 °C, respectively. The SANS experiment almost covers the entire nanometer range because the q -range from 0.01 to 3 nm⁻¹ corresponds to real-space periodicities between 2 and 600 nm. Liposomes, however, have aperiodic spacing and, thus, the maximum liposome diameter, that can be determined, is given by $\pi/q_{\min} \approx 300$ nm. Therefore, only some of the liposomal suspensions can be characterized with respect to the liposome size, but the SANS data allow measuring the lipid bilayer thickness for all of them.

The bilayer thickness of the selected liposomes for the medically relevant temperature range is compiled in Tables 2 and 3. As expected, the liposomes with a transition temperature above 42 °C do not exhibit any change in bilayer thickness. Pes-PC-Pes and Pad-PC-Pad liposomes, however, show the tendency for losing interdigitation of the lipid bilayers already well below T_m .

Table 2. Most Probable¹⁵ Bilayer Thickness (nm) of the Selected Liposomes as a Function of Temperature^a

phospholipid	temperature, °C							
	22	25	28	32	35	39	42	22
DPPC	4.6	4.6	4.6	4.6	4.6	4.7	4.7	4.7
Rad-PC-Rad	4.6	4.6	4.6	4.5	4.5	4.4	4.4	4.5
Pad-Pad-PC	5.6	5.6	5.6	5.5	5.5	5.6	5.6	5.7
Pes-PC-Pes	3.9	4.2	4.5	4.4	4.6	4.7	4.6	4.8
Sur-PC-Sur	3.1	3.1	3.1	3.1	3.1	3.1	3.1	3.1
Sad-PC-Sad	3.2	3.5	3.5	3.5	3.5	3.4	3.3	3.0

^aThe goodness of the fit, described by reduced chi-square, varies between 3 and 15.

The well-established DPPC liposomes were incorporated into the study for comparison. The decrease of forward scattered intensity for DPPC with increasing temperature is likely caused by increasing repulsive interactions associated with the pre-transition temperature of DPPC, which varies between 33.5 and 35.8 °C, and is even 37.4 °C in case of the use of D₂O.²⁵ This hypothesis has to be verified by a future study. The mean size of the DPPC liposomes, as derived from cryo-TEM images and represented exemplarily in Figure 1A, was (87 ± 20) nm, and about 16% of them were multi-lamellar. The SANS data of Pes-PC-Pes liposomes, see Figure

Table 3. Structural Data Derived from SANS Demonstrate the Pad-PC-Pad Liposome Shape Changes Close to T_m ^a

temperature, °C	radius, nm	eccentricity	bilayer thickness, nm	reduced chi-square
22	70 ± 19	0.35	3.5 ± 1.1	18.9
25	66 ± 21	0.35	3.4 ± 0.9	18.1
28	70 ± 16	0.32	3.3 ± 0.9	22.4
32	70 ± 16	0.31	3.4 ± 0.9	21.7
35	70 ± 7 (65)	0.1 (0.88)	3.3 ± 0.7 (3.4 ± 0.9)	178.7 (19.2)
39	72 ± 5	0.04	3.4 ± 0.8	17.5
42	71 ± 5	0.05	3.6 ± 0.7	107.1
22	70 ± 32	0.04	4.2 ± 0.7	9.4

^aAt a temperature of 35 °C, the contribution for discs with homogeneous cross-section was accounted for—values in brackets.

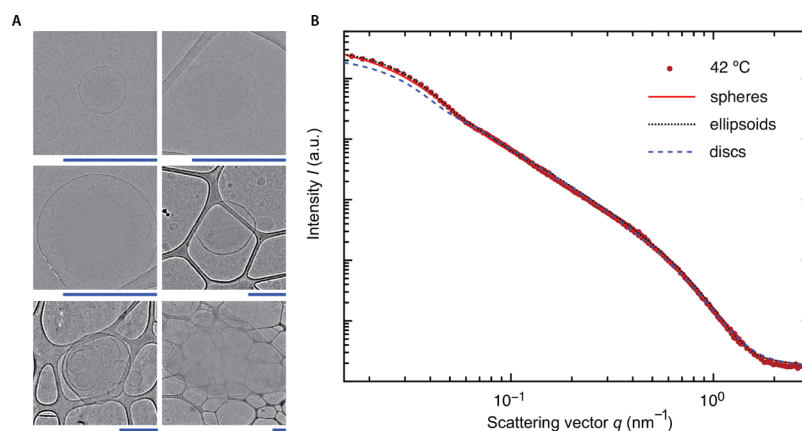


Figure 3. (A) Exemplified cryo-TEM images verify the manifold shapes and sizes of the Rad-PC-Rad liposomes used. The scale bars correspond to a length of 500 nm. (B) Discs less suitably describe the SANS data of Rad-PC-Rad liposomes than the ellipsoidal and spherical models.

1B, indicate the presence of two liposome populations with sizes of about 100 and 1000 nm—no plateau at low q -values and of stacked lipid bilayers—prominent BRAGG peak at $q = 0.83 \text{ nm}^{-1}$. Increasing the temperature, the peak gradually diminishes associated with the disintegration of the stacked lipid bilayers.

The fitting of the SANS data for Pad-PC-Pad liposomes was especially challenging. Therefore, not only the bilayer thickness was determined but also their radius and eccentricity. The radius was not affected by the temperature cycle, whereas the eccentricity abruptly changed already well below the transition temperature, i.e. between 32 and 35 °C. This change in shape, however, is not linked with the increase of the bilayer thickness, which has been observed after cooling-down to room temperature. The shape change of Pad-PC-Pad liposomes from ellipsoidal or better faceted entities to discs as the result of the heating was validated by the cryo-TEM images, exemplarily displayed in Figure 1C.

For Rad-PC-Rad, Pad-Pad-PC, Sur-PC-Sur, and Sad-PC-Sad liposomes, the q -plots derived coincide, which proves their thermal stability within the medically relevant temperature range. The fitting of SANS data for Rad-PC-Rad liposomal suspensions was challenging, easily explained by the presence of their size and shape distributions indicated in the micrographs of Figure 3A. Figure 3B exemplarily summarizes the fitting of the data obtained at a temperature of 42 °C. Ignoring the inter-particle interactions and considering ellipsoid shape, one can find a better approximation than for the discoid model. The goodness of fit, described by reduced chi-square, is for spheres 11.4, for ellipsoids 30.3, and for discs 47.8. The thermal stability of the Rad-PC-Rad liposomes with their wide-spread size and shape distribution within the

medically relevant temperature range, however, is the key observation and more essential than the selection of the most appropriate model.

DISCUSSION AND CONCLUSIONS

The bilayer thickness of the DPPC liposomes derived in this study perfectly agrees with the values reported,^{26,27} which indicates an appropriate fitting procedure. The liposomes of Pes-PC-Pes, also known as β -DPPC, exhibit interdigitated lipid bilayer in the gel phase but not in the liquid crystalline phase.²⁸ Therefore, the phase transition results in a bilayer thickness increase by 20%²⁸—a value consistent with the present study. The study also shows that the changes in the tail-to-tail van der Waals forces and inter-head-group hydrogen bonding in the series from Pad-Pad-PC via Sur-PC-Sur to Sad-PC-Sad do hardly affect the overall properties of the liposomes. Likewise, Pad-PC-Pad lipids are interdigitated below T_m and lose this structural property at higher temperatures.^{3,8} In agreement with the present study, recent SAXS data have indicated that the head-to-head distance of Pad-PC-Pad bilayer increases as the result of mechanical stimuli.⁵ The observed 20% increase in bilayer thickness after heating above T_m denotes thermally induced structural changes. These structural changes of Pad-PC-Pad liposomes within the physiologically relevant temperature range is counter-indicative of its use as a carrier for targeted drug delivery in humans.

The C17 homologue of Pad-PC-Pad, that is, Rad-PC-Rad, which features a higher transition temperature,⁶ should allow for mechanically responsive drug delivery within the human body. Although the used Rad-PC-Rad liposomes possess a wide variety of sizes and shapes, they show the structural stability at the level of the bilayer membrane in the

physiologically relevant temperature range between 22 and 42 °C.

AUTHOR INFORMATION

Corresponding Author

*E-mail: bert.mueller@unibas.ch.

ORCID

Bert Müller: 0000-0003-4078-9109

Present Address

^{||}Institute of Sound and Vibration Research (ISVR), University of Southampton, Highfield, Southampton, SO17 1BJ, UK.

Author Contributions

The study was designed by A.Z. The samples were prepared by F.N. The SANS experiments were carried out by J.K., A.Z., F.N., and S.M. The data analysis and interpretation were mainly performed by J.K., H.D., and S.M. with the active support of B.M. The manuscript including the figures and tables were compiled by S.M. and B.M. All authors have given approval to the final version of the manuscript.

Funding

S.M. obtained financial support from the Swiss Government Excellence Scholarship Program for a period of 36 months. The study is partially based on the funding by the Swiss National Science Foundation (SNSF) via the National Research Program (NRP) 62 “Smart Materials”. A.Z. was financially supported by the Swiss National Science Foundation through a Professorial Fellowship.

Notes

The authors declare no competing financial interest.

ACKNOWLEDGMENTS

S.M. acknowledges the financial support of the Swiss Government via the Excellence Scholarship Program for Foreign Scholars and Artists (2015-2018). The authors are grateful to the funding provided by the Swiss National Science Foundation (SNSF) within project #126090. The authors thank the Paul Scherrer Institute, Villigen (Switzerland) for beamtime and the Bio-EM Lab (Biozentrum, University of Basel, Switzerland) for the cryo-TEM support as well as Takashi Ishikawa, Villigen, Switzerland for the early discussion of cryo-TEM results. The support of Georg Schulz, Basel, Switzerland for the background correction of the micrographs in Figure 3 is gratefully acknowledged.

ABBREVIATIONS

cryo-TEM, cryogenic transmission electron microscopy; DLS, dynamic light scattering; DPPC, 1,2-dipalmitoyl-*sn*-glycero-phosphocholine; Pad-Pad-PC, 1,2-dipalmityl-amido-glycero-3-phosphocholine; Pad-PC-Pad, 1,3-dipalmityl-amido-glycero-2-phosphocholine; PDI, polydispersity index; Rad-PC-Rad, 1,3-dihexadecyl-amido-glycero-phosphocholine; SANS, small-angle neutron scattering; SAXS, small-angle X-ray scattering; Sad-PC-Sad, 1,3-distearoyl-amido-glycero-phosphocholine; Sur-PC-Sur, 1,3-dihexadecyl-urea-glycero-2-phosphocholine

REFERENCES

- (1) Allen, T. M.; Cullis, P. R. Liposomal Drug Delivery Systems: From Concept to Clinical Applications. *Adv. Drug Delivery Rev.* **2013**, *65*, 36–48.
- (2) Zumbuehl, A. Artificial Phospholipids and Their Vesicles. *Langmuir* **2018**, DOI: 10.1021/acs.langmuir.8b02601.

- (3) Holme, M. N.; Fedotenko, I. A.; Abegg, D.; Althaus, J.; Babel, L.; Favarger, F.; Reiter, R.; Tanasescu, R.; Zaffalon, P.-L.; Ziegler, A.; Müller, B.; Saxer, T.; Zumbuehl, A. Shear-Stress Sensitive Lenticular Vesicles for Targeted Drug Delivery. *Nat. Nanotechnol.* **2012**, *7*, 536–543.

- (4) American Heart Association, Guidelines for Cardiopulmonary Resuscitation and Emergency Cardiovascular Care. *Circulation* **2005**, *112*, IV1-IV205.

- (5) Buscema, M.; Deyhle, H.; Pfohl, T.; Zumbuehl, A.; Müller, B. Spatially resolved small-angle X-ray scattering for characterizing mechanoresponsive liposomes using microfluidics. *Mater. Today Bio* **2019**, *1*, 100003.

- (6) Neuhaus, F.; Mueller, D.; Tanasescu, R.; Balog, S.; Ishikawa, T.; Brezesinski, G.; Zumbuehl, A. Synthesis and Biophysical Characterization of an Odd-Numbered 1,3-Diamidophospholipid. *Langmuir* **2018**, *34*, 3215–3220.

- (7) Neuhaus, F.; Mueller, D.; Tanasescu, R.; Stefanu, C.; Zaffalon, P.-L.; Balog, S.; Ishikawa, T.; Reiter, R.; Brezesinski, G.; Zumbuehl, A. Against the Rules: Pressure Induced Transition from High to Reduced Order. *Soft Matter* **2018**, *14*, 3978–3986.

- (8) Weinberger, A.; Tanasescu, R.; Stefanu, C.; Fedotenko, I. A.; Favarger, F.; Ishikawa, T.; Brezesinski, G.; Marques, C. M.; Zumbuehl, A. Bilayer Properties of 1,3-Diamidophospholipids. *Langmuir* **2015**, *31*, 1879–1884.

- (9) Neuhaus, F.; Mueller, D.; Tanasescu, R.; Balog, S.; Ishikawa, T.; Brezesinski, G.; Zumbuehl, A. Vesicle Origami: Cuboid Phospholipid Vesicles Formed by Template-Free Self-Assembly. *Angew. Chem.* **2017**, *129*, 6615–6618.

- (10) Walde, P. Preparation of Vesicles (Liposomes). *Encyclopedia of Nanoscience and Nanotechnology*; American Scientific Publishers, 2004; Vol. 8, pp 43–79.

- (11) Schulz, G.; Waschkes, C.; Pfeiffer, F.; Zanette, I.; Weitkamp, T.; David, C.; Müller, B. Multimodal Imaging of Human Cerebellum—Merging X-Ray Phase Microtomography, Magnetic Resonance Microscopy and Histology. *Sci. Rep.* **2012**, *2*, 826.

- (12) Ahmed, M. N.; Yamany, S. M.; Mohamed, N.; Farag, A. A.; Moriarty, T. A Modified Fuzzy C-Means Algorithm for Bias Field Estimation and Segmentation of MRI Data. *IEEE Trans. Med. Imaging* **2002**, *21*, 193–199.

- (13) Keiderling, U. The New “BerSANS-PC” Software for Reduction and Treatment of Small Angle Neutron Scattering Data. *Appl. Phys. A: Mater. Sci. Process.* **2002**, *74*, s1455–s1457.

- (14) Strunz, P.; Saroun, J.; Keiderling, U.; Wiedenmann, A.; Przenioslo, R. General Formula for Determination of Cross-Section from Measured SANS Intensities. *J. Appl. Crystallogr.* **2000**, *33*, 829–833.

- (15) Breßler, I.; Kohlbrecher, J.; Thünemann, A. F. SASfit: a tool for small-angle scattering data analysis using a library of analytical expressions. *J. Appl. Crystallogr.* **2015**, *48*, 1587–1598.

- (16) Guiner, A.; Fournet, G.; Walker, C. *Small Angle Scattering of X-Rays*; Jahn Willey-Champan: New York, 1955.

- (17) Baxter, R. J. Percus-Yevick Equation for Hard Spheres with Surface Adhesion. *J. Chem. Phys.* **1968**, *49*, 2770–2774.

- (18) De Kruijff, C. G. Adhesive Hard-Sphere Colloidal Dispersions. A Small-Angle Neutron-Scattering Study of Stickiness and the Structure Factor. *Langmuir* **1989**, *5*, 422–428.

- (19) Hjelm, R. P.; Schteingart, C. D.; Hofmann, A. F.; Thiyagarajan, P. Structure of Conjugated Bile Salt–Fatty Acid–Monoglyceride Mixed Colloids: Studies by Small-Angle Neutron Scattering. *J. Phys. Chem. B* **2000**, *104*, 197–211.

- (20) Fratzl, P. Statistical Model of the Habit and Arrangement of Mineral Crystals in the Collagen of Bone. *J. Stat. Phys.* **1994**, *77*, 125–143.

- (21) Pedersen, J. S. Modelling of Small-Angle Scattering Data from Colloids and Polymer Systems. *Neutrons, X-rays and Light*; Elsevier, 2002; pp 391–420.

- (22) Schwartz, S.; Cain, J. E.; Dratz, E. A.; Blasie, J. K. An Analysis of Lamellar X-Ray Diffraction from Disordered Membrane Multilayers

with Application to Data from Retinal Rod Outer Segments. *Biophys. J.* **1975**, *15*, 1201–1233.

(23) Frühwirth, T.; Fritz, G.; Freiburger, N.; Glatter, O. Structure and Order in Lamellar Phases Determined by Small-Angle Scattering. *J. Appl. Crystallogr.* **2004**, *37*, 703–710.

(24) Tanasescu, R.; Lanz, M. A.; Mueller, D.; Tassler, S.; Ishikawa, T.; Reiter, R.; Brezesinski, G.; Zumbuehl, A. Vesicle Origami and the Influence of Cholesterol on Lipid Packing. *Langmuir* **2016**, *32*, 4896–4903.

(25) Matsuki, H.; Okuno, H.; Sakano, F.; Kusube, M.; Kaneshina, S. Effect of Deuterium Oxide on the Thermodynamic Quantities Associated with Phase Transitions of Phosphatidylcholine Bilayer Membranes. *Biochim. Biophys. Acta, Biomembr.* **2005**, *1712*, 92–100.

(26) Nele, V.; Holme, M. N.; Kauscher, U.; Thomas, M. R.; Douth, J. J.; Stevens, M. M. Effect of Formulation Method, Lipid Composition, and PEGylation on Vesicle Lamellarity: A Small-Angle Neutron Scattering Study. *Langmuir* **2019**, *35*, 6064–6074.

(27) Nagle, J. F.; Tristram-Nagle, S. Structure of Lipid Bilayers. *Biochim. Biophys. Acta, Rev. Biomembr.* **2000**, *1469*, 159–195.

(28) Serrallach, E. N.; Dijkman, R.; De Haas, G. H.; Shipley, G. G. Structure and thermotropic properties of 1,3-dipalmitoyl-glycero-2-phosphocholine. *J. Mol. Biol.* **1983**, *170*, 155–174.